

Geomaterials (Petrology)  
Genesis of adakite-like lavas of Licancabur volcano  
(Chile—Bolivia, Central Andes)

Oscar Figueroa<sup>a</sup>, Bernard Déruelle<sup>b,\*</sup>, Daniel Demaiffe<sup>c</sup>

<sup>a</sup>Departamento Ciencias de la Tierra, Universidad de Concepción, Casilla 160-C, Concepción, Chili

<sup>b</sup>UMR 7154, laboratoire de magmatologie et géochimie inorganique et expérimentale,  
institut de physique du globe de Paris, université Pierre-et-Marie-Curie, 4, place Jussieu,  
75252 Paris cedex 05, France

<sup>c</sup>Laboratoire de géochimie isotopique, université libre de Bruxelles (ULB),  
50, avenue F.D.-Roosevelt, CP 160/02, 1050 Brussels, Belgium

Received 23 January 2008; accepted after revision 18 November 2008

Available online 28 February 2009

Presented by Claude Jaupart

## Abstract

The Licancabur volcano is located on the Bolivia—Chile Altiplano (Central Andes). The lavas are andesites and dacites. Numerous mineralogic features attest that magma mixing occurred. Andesites have concave (spoon-shaped) REE patterns whereas dacites have steep slopes. A spectacular crossover of patterns occurs with increasing SiO<sub>2</sub>. Most geochemical discrimination criteria of adakites are satisfied by Licancabur dacites, except their high Sr-isotope compositions (> 0.7075). For the genesis of the Licancabur adakite-like lavas, a four-step model is proposed: (1) partial melting (5 to 10 wt %) of a subducted altered oceanic crust; (2) hybridation (< 10 wt %) of the magmas with melts derived from the overlying lithospheric mantle; (3) contamination (≈ 1 wt %) of these hybrid magmas by TTG-type granodiorites of the Archean lower continental crust (with present-day Sr-isotope ratios ≈ 0.820); (4) evolution and differentiation by crystal fractionation (< 6 wt %) and magma mixing at upper crustal levels. **To cite this article:** O. Figueroa et al., *C. R. Geoscience* 341 (2009).

© 2008 Académie des sciences. Published by Elsevier Masson SAS. All rights reserved.

## Résumé

**Genèse des laves à tendance adakitique du volcan Licancabur (Chili—Bolivie, Andes centrales).** Le volcan Licancabur est situé sur l'Altiplano bolivo-chilien (Andes centrales). Ses laves sont des andésites et dacites. De nombreux critères minéralogiques permettent de mettre en évidence des mélanges magmatiques. Les spectres de terres rares sont concaves pour les andésites, pentus pour les dacites et se croisent avec les teneurs en SiO<sub>2</sub> croissantes. Les critères définissant les adakites sont satisfaits pour les dacites du Licancabur, sauf pour les valeurs élevées des rapports isotopiques du Sr (> 0.7075). Un modèle en quatre étapes est proposé pour la genèse des laves : (1) la fusion partielle (5 à 10 % en masse) de la croûte océanique subductée altérée ; (2) l'hybridation (< 10 % en masse) par des magmas issus du manteau lithosphérique sus-jacent ; (3) la contamination (≈ 1 % en masse) des magmas hybrides par des granodiorites archéennes de type TTG de la croûte continentale inférieure ; (4) l'évolution par cristallisation fractionnée

\* Corresponding author.

E-mail addresses: [ofiguero@udec.cl](mailto:ofiguero@udec.cl) (O. Figueroa), [deruelle@ipgp.jussieu.fr](mailto:deruelle@ipgp.jussieu.fr) (B. Déruelle), [ddemaif@ulb.ac.be](mailto:ddemaif@ulb.ac.be) (D. Demaiffe).

(jusqu'à 6 % en masse) et mélanges magmatiques dans la croûte supérieure. *Pour citer cet article : O. Figueroa et al., C. R. Geoscience 341 (2009).*

© 2008 Académie des sciences. Publié par Elsevier Masson SAS. Tous droits réservés.

**Keywords:** Licancabur volcano; Central Andes; Andesites; Dacites; Adakite-like lavas; Central Andes

**Mots clés :** Volcan Licancabur ; Andes centrales ; Andésites ; Dacites ; Tendance adakitique ; Andes centrales

### 1. Introduction

The Licancabur volcano is located on the western border of the Bolivia—Chile Altiplano (Fig. 1). It belongs to the southern part of the Andean Central Volcanic Zone (CVZ). It was mostly built up after the Late Glacial period (12–10 ka [18]) and rests upon the 1.35 Ma old Purico ignimbrites [11]. Three major lithological units (lower, intermediate and upper,

respectively) are distinguished according to the stratigraphy [12]. They correspond to:

- oldest lava flows, possibly covered by piedmont, moraine, and avalanche deposits at the bottom of the volcano;
- dominant lava flows which built up most of the cone;
- summit lava flows and pyroclastic deposits.

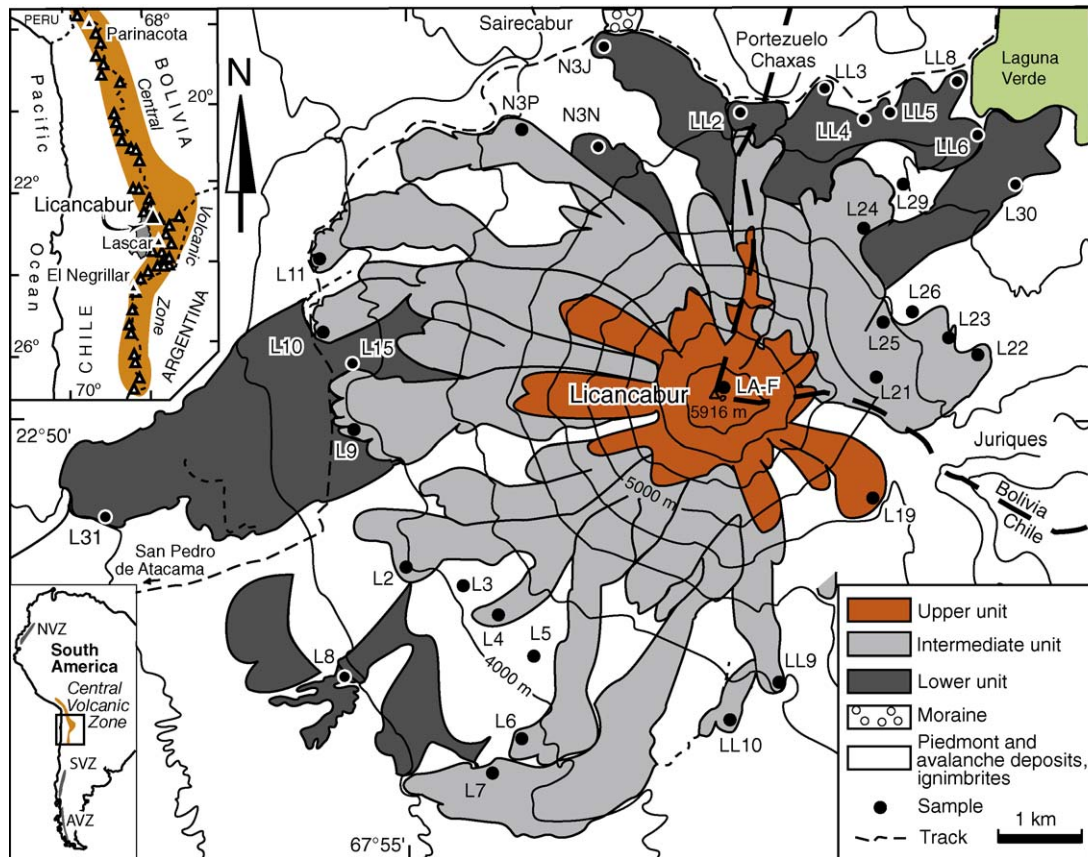


Fig. 1. Location of Licancabur volcano in the Andean Central Volcanic Zone. Lower inset: the four Andean volcanic zones (NVZ: 5°N–2°S, CVZ: 14°S–27°S, SVZ: 33°S–46°S, AVZ: 49°S–55°S, northern, central, southern, and austral Volcanic Zones, respectively). Upper inset: the main volcanoes of the CVZ south of 17°S.

Fig. 1. Localisation du volcan Licancabur dans la zone volcanique des Andes centrales ; en cartouche bas: les quatre zones volcaniques andines (NVZ : 5°N–2°S, CVZ : 14°S–27°S, SVZ : 33°S–46°S et AVZ : 49°S–55°S, zones septentrionale, centrale, méridionale et australe, respectivement) et haut : la CVZ au sud de 17°S.

## 2. Petrography and mineralogy

The Licancabur andesites and dacites (Fig. 2) are less porphyritic (< 12 vol% phenocryst) than most lavas from other volcanoes in the CVZ, such as Lascar ([8], Fig. 1). Their texture is seriate with a hyalopilitic groundmass. The phenocrysts (> 1 mm) are plagioclase, orthopyroxene, clinopyroxene, olivine, amphibole and Ti-magnetite. Gabbro xenoliths are common: they consist either of the assemblage Pl + Cpx + Opx + Ti-Mag + pargasite relicts in an interstitial glass including tiny acicular microlites of clinopyroxene, or of plagioclase phenocrysts (2 to 7 mm-long; up to 9 vol%) arranged in synneusis texture.

In andesites, olivine phenocrysts (up to 5 mm) contain Ti-magnetite and chromite inclusions. The Fo content decreases slightly but significantly from Fo<sub>82</sub> to Fo<sub>67</sub> with increasing SiO<sub>2</sub> contents of the host lavas. Olivine xenocrysts, sometimes surrounded by an orthopyroxene corona, are richer in Mg (Fo<sub>87</sub>). Plagioclase phenocrysts (up to 3 mm) are euhedral, limpid, mainly normally zoned; some are sieve-textured with core compositions varying from An<sub>82</sub> to An<sub>55</sub> in a single lava. Two populations of orthopyroxene phenocrysts (up to 1.7 mm) with distinct En (84 and 63 ± 3) and mg# (0.77 and 0.68 ± 0.02) are present in a given lava sample. Clinopyroxene phenocrysts (84 > mg# > 68) are ubiquitous and sometimes embayed. Tiny amphibole

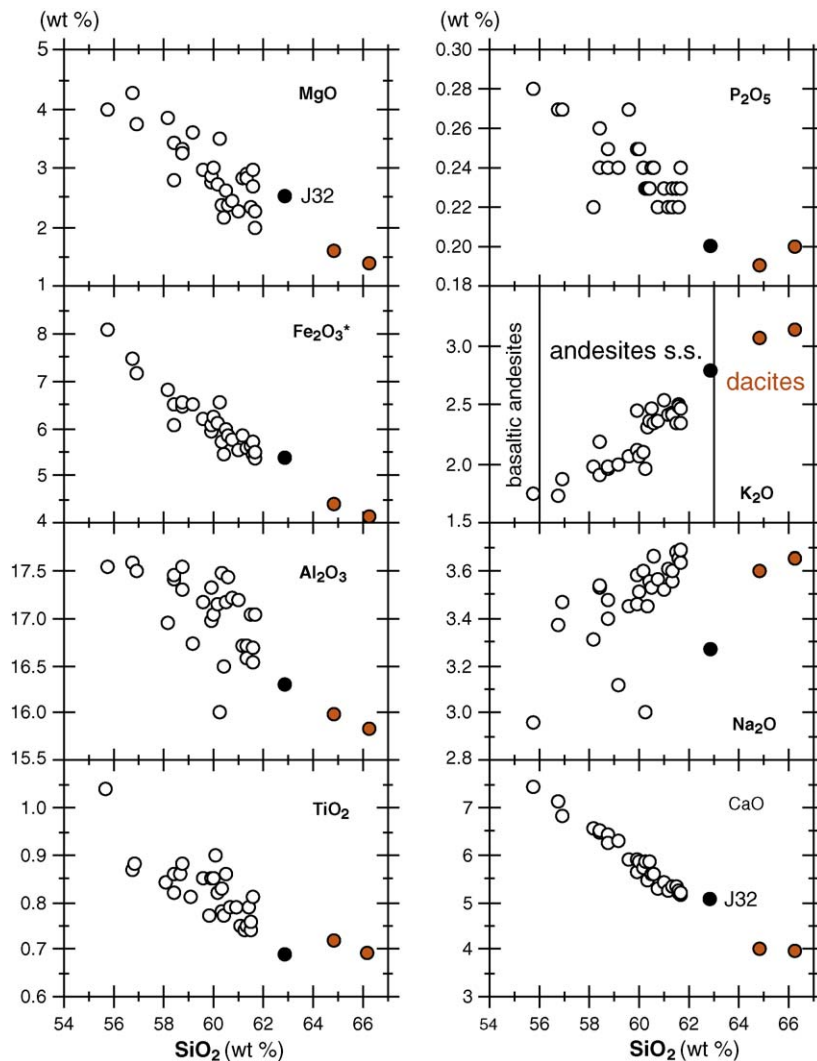


Fig. 2. Harker diagrams for Licancabur lavas. The nomenclature of the lavas is indicated in the SiO<sub>2</sub>–K<sub>2</sub>O diagram. Purico ignimbrite J32 is also plotted.

Fig. 2. Diagrammes de Harker pour les laves du Licancabur. La terminologie des laves utilisée est indiquée dans le diagramme SiO<sub>2</sub>–K<sub>2</sub>O. L'ignimbrite de Purico J32 est indiquée.

microphenocrysts (Mg-hornblende to tschermakite, nomenclature after [19]) have high  $\text{Al}_2\text{O}_3$  content (7.0 to 11.0 wt %). They are often surrounded by a rim of Fe—Ti oxides or by reaction rims composed of pyroxene + plagioclase + Ti-magnetite.

In dacites, plagioclase ( $\approx 0.3$  mm), clinopyroxene ( $\text{mg}\# = 0.76$ ), orthopyroxene ( $\text{mg}\# = 0.67$ ) and rare biotite microphenocrysts occur. Rare hornblende phenocrysts (Mg-hornblende to tschermakite) are scattered in the glassy matrix.

All lavas contain phenocrysts of Fe—Ti oxides, Ti-magnetite being more common than ilmenite. The matrix contains microlites of plagioclase, pyroxenes and Fe—Ti oxides; its  $\text{SiO}_2$  content increases from 65 to 78 wt % from andesites to dacites.

Calculated temperatures for coexisting Fe—Ti oxide pairs are between 860 and  $1060 \pm 20$  °C for andesites, around  $930 \pm 20$  °C for dacites. Oxygen fugacity estimates (at  $930 \pm 20$  °C) are higher for dacites ( $-9 > \log f\text{O}_2 > -10$ ) than for andesites ( $-10 > \log f\text{O}_2 > -12$ ). Temperatures estimated for coexisting clinopyroxene and orthopyroxene phenocryst pairs range between 920 et 1090 °C, higher equilibrium temperatures being observed for rims (difference up to 150 °C). Pressure estimate for amphibole relicts in gabbroic xenoliths ( $0.59 \pm 0.01$  GPa) is higher than for phenocrysts ( $0.28$  to  $0.36 \pm 0.03$  GPa).

Representative analyses of minerals can be obtained from the corresponding author upon request.

### 3. Geochemistry

Representative lavas (33 samples) of Licancabur have been analyzed for major and trace elements by ICP and ICP—MS (CRPG—CNRS, Nancy, France; analytical conditions [10]) and for isotopes at the Laboratoire de géochimie isotopique, ULB, Bruxelles, Belgium (analytical conditions [1]). Chemical analyses can be obtained upon request from the corresponding author. Results are presented in Figs. 2 and 3.

Major elements are generally well correlated with  $\text{SiO}_2$ ; most elements decrease with increasing silica, except  $\text{Na}_2\text{O}$  and  $\text{K}_2\text{O}$ . Correlations are also good for trace elements: incompatible elements (Rb, Ba, Cs, Th, U, Pb, Ta, Nb, Zr, Hf) increase, whereas compatible elements (V, Co, Sc) decrease with increasing differentiation. The scattering observed for Cr and Ni (Fig. 3) can be explained by the occurrence of olivine xenocrysts (2 vol %) with chromite or Cr-spinel inclusions. Removal of up to 2 wt % olivine (Ni  $\approx 0.5$  wt %) or up to 0.2 wt % chromite put the scattered samples back along the main lava trend.

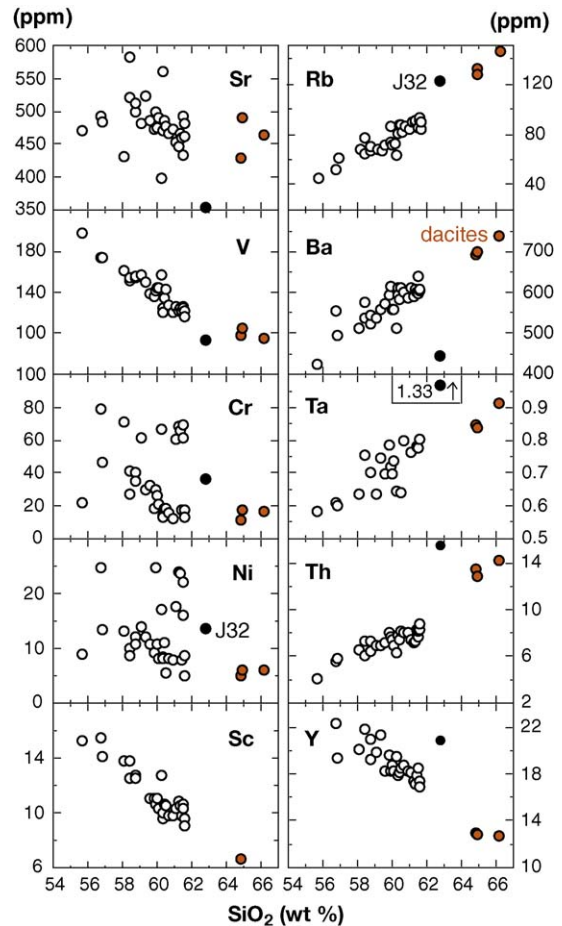


Fig. 3. Trace element distribution in Licancabur lavas according to their  $\text{SiO}_2$  content. Purico ignimbrite J32 is also plotted.

Fig. 3. Distribution des éléments en traces dans les laves du Licancabur en fonction des teneurs en  $\text{SiO}_2$ . L'ignimbrite de Purico J32 est indiquée.

Nevertheless, the dacites generally plot apart the andesite trends. Andesites have concave REE patterns whilst dacites have steep slopes (Fig. 4). For the series as a whole, the light REE (La—Sm) contents increase meanwhile heavy REE (Gd—Lu) ones decrease with increasing  $\text{SiO}_2$  resulting in spectacular pattern cross-over. The La/Yb ratio increases from 10.3 in basaltic andesite L31 to 44.3 in dacite L19. All the lavas present a small negative europium anomaly ( $[\text{Eu}/\text{Eu}^*]_{\text{N}} \approx 0.8$ ). The dacites have low Y and high Sr contents, when compared to the andesites, giving them an adakitic trend [6] (Fig. 5). Isotopic compositions ( $0.70760 < {}^{87}\text{Sr}/{}^{86}\text{Sr} < 0.70861$ ;  $-6.2 > \varepsilon\text{Nd} > -7.6$ ;  $18.781 < {}^{206}\text{Pb}/{}^{204}\text{Pb} < 18.852$ ;  $15.662 < {}^{207}\text{Pb}/{}^{204}\text{Pb} < 15.692$ ;  $38.792 < {}^{208}\text{Pb}/{}^{204}\text{Pb} < 38.891$ ) fall into the range established for other volcanoes of CVZ [16,17].

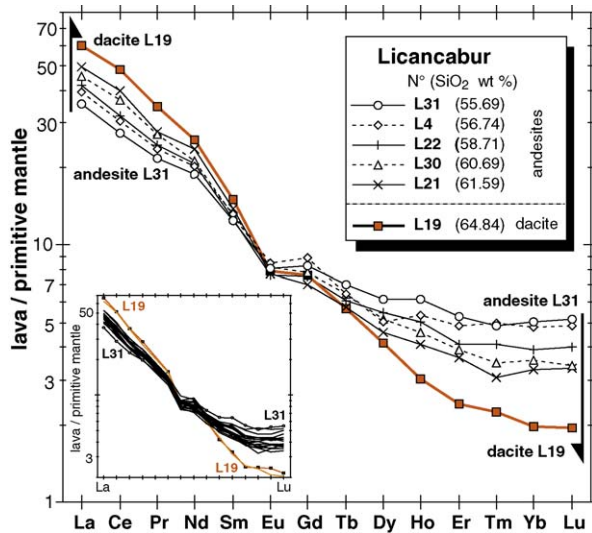


Fig. 4. Primitive mantle [23] rare earth normalized abundance diagram for Licancabur representative lavas. The silica contents of the selected samples (wt %) are indicated. Inset: patterns for studied Licancabur lavas.

Fig. 4. Diagramme d'abondance des terres rares normalisées au manteau primitif [23] pour les laves du volcan Licancabur. La teneur en silice (% en poids) des échantillons sélectionnés est indiquée. Les flèches indiquent l'évolution des teneurs en terres rares avec la silice croissante. En cartouche : spectres des laves du Licancabur étudiées.

#### 4. Adakite-like dacites of Licancabur

Andesites from Licancabur are not “true” adakites, as defined by Defant and Drummond [6], due to their high Y and Yb contents (resulting in low La/Yb ratios) and to high Sr and low Nd isotope ratios (Table 1). Nevertheless, they have Sr (and Y) contents similar to those of these rocks (Fig. 5). They are quite comparable to lavas from Antisana volcano (NVZ, Fig. 1) which were qualified of adakite-like lavas [3]. “True” adakites [6] are present in the CVZ, at El Negrillar (B.D. unpublished data; Fig. 1). Most geochemical major and trace element discrimination criteria used in the definition of adakites ([6], Table 1) are satisfied by Licancabur dacites, except the Sr- and Nd-isotope compositions that are, respectively, higher than 0.7045 and lower than 0.5129.

#### 5. Discussion

The genesis of the primary magmas of the Licancabur volcano is discussed in terms of partial melting of the subducted oceanic slab, of magma and associated hydrous fluids ascent and evolution upwards through the lithospheric mantle wedge and through the lower and upper continental crust, till lava eruption in

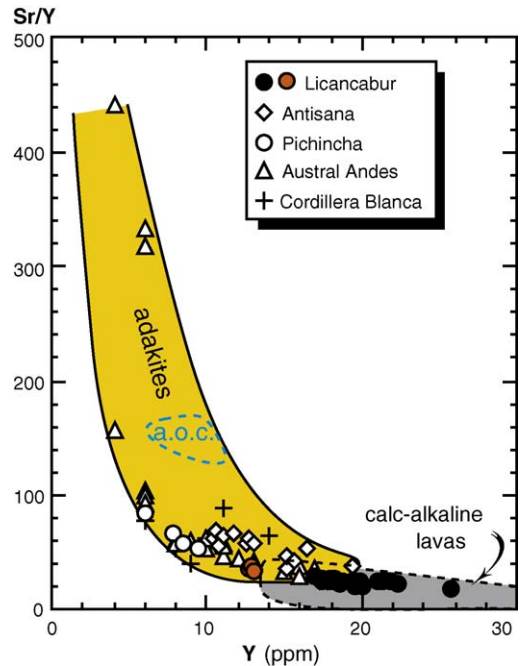


Fig. 5. Y—Sr/Y diagram for Licancabur lavas. Selected lavas from Antisana [3], Pichincha [2], AVZ [27] and granodiorites from the Cordillera Blanca batholith, Peru, [24] are also plotted. Fields for adakites and calc-alkaline lavas [6], and for experimental melting of altered oceanic crust (aoc) [26] are indicated.

Fig. 5. Diagramme Y—Sr/Y pour les laves du Licancabur. Sont aussi indiquées des laves des volcans Antisana [3], Pichincha [2] (NVZ), de l'AVZ [27] et des granodiorites du batholithe miocène de la Cordillera Blanca au Pérou [24]. Les domaines des adakites et des laves calc-alkalines [6] et des liquides provenant de la fusion partielle expérimentale [26] d'un basalte de croûte océanique altérée (aoc) sont indiqués.

Table 1

Geochemical characteristics of Licancabur lavas compared to those of adakites [6]. Numbers in italics differ from characteristics of adakites. Tableau 1

Caractéristiques géochimiques des laves du Licancabur comparées à celles des adakites [6]. Les nombres en italics diffèrent des caractéristiques des adakites.

	Adakites [6]	Licancabur andesites	Dacites
wt %			
SiO <sub>2</sub>	> 56	56–62	62–66
Al <sub>2</sub> O <sub>3</sub>	> 15	16.5–17.6	15.8–16.0
MgO	< 3	2.0–4.3	1.4–1.6
Na <sub>2</sub> O	3.5–7.5	3.0–3.7	3.5–3.6
mg#	> 0.36	0.42–0.53	0.40–0.42
ppm			
Sr	> 400	400–580	430–490
Y	< 18	16.9–25.8	12.7–13.0
Yb	< 1.8	1.37–2.23	0.87–0.93
La/Yb	> 20	10.3–22.2	41.2–44.3
<sup>87</sup> Sr/ <sup>86</sup> Sr	< 0.7045	0.7076–0.7083	0.7086
<sup>143</sup> Nd/ <sup>144</sup> Nd	> 0.5129	0.5123–0.5132	0.5123

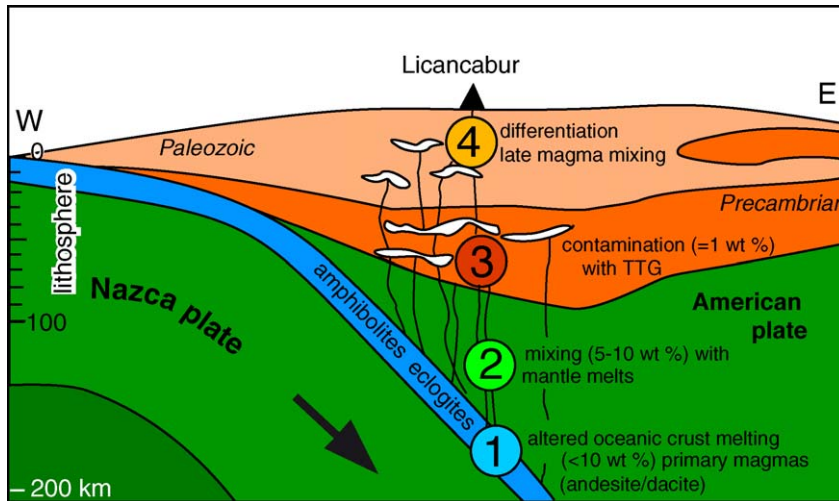


Fig. 6. Model of genesis of Licancabur lavas (see text for explanations).

Fig. 6. Modèle de genèse des laves du Licancabur (voir le texte).

the Andean cordillera (Fig. 6). Similar hypotheses have been presented for the genesis of Andean adakites from the NVZ [2,3] and AVZ [27]. Whereas sediment contribution and northwards increasing of continental crust contribution have been invoked for the genesis of adakites from the AVZ [27], the role of continental crust is ruled out in the NVZ [2,3].

### 5.1. Genesis of primary magmas (andesites—dacites) by partial melting of garnet amphibolites and/or amphibole eclogites of the subducted oceanic crust: the key to concave (spoon-shape) and crossover REE patterns

Experiments [15] have shown that primary calc-alkaline magmas can be produced by partial melting of tholeiitic basalts of the subducted oceanic crust leaving a residual assemblage of clinopyroxene  $\pm$  garnet  $\pm$  amphibole, or of pyroxenes  $\pm$  garnet  $\pm$  Ca-plagioclase according to mostly dry or wet prevailing conditions. More recently, this hypothesis has been proposed for the study of adakites [6]. At Licancabur, the concave REE patterns of andesites imply fractionation of amphibole and the crossover of REE patterns observed for the whole series implies fractionation of garnet. The simultaneous occurrence of these two minerals is typical of garnet amphibolites and/or amphibole eclogites. The pressure required to obtain these rocks during subduction is in the range 1.5–3.0 GPa, corresponding to depths of 50–100 km. The top of the subducted slab beneath Licancabur is located at  $90 \pm 10$  km depth. Assuming a convergence rate of  $6\text{--}10 \text{ cm.y}^{-1}$ , the age of the subducted oceanic crust at

this depth below the southern CVZ is Eocene with a temperature of its upper part between 700 and 1000 °C [28,29]. The oceanic crust is then metamorphosed into eclogite + metastable metagabbro + hydrous phases assemblage. So the first stage in the genesis of Licancabur magmas could consist of partial melting ( $\approx 5 \text{ wt } \%$ ) of an altered oceanic crust [26], metamorphosed into garnet amphibolites and/or amphibole eclogites with a Hbl + Cpx + Grt + Pl + oxides (62:20:10:5:3) residuum for andesites and a Grt + Hbl + Pl (61:35:4) residuum for dacites (partition coefficients after [14]). Calculated/measured REE abundance ratios for dacites are between 0.8 and 1.2. The respective proportions of garnet and amphibole and the garnet composition ( $\text{Prp}_{55}\text{Alm}_{25}\text{Sp}_{820}$ ) determine the andesitic or dacitic character of each magma batch ( $\text{SiO}_2$  content and REE distribution).

Another possible hypothesis is to consider that melting of basalts under amphibolite—eclogite facies occurs at the bottom of the continental crust. Such basalts may have been underplated during subduction or emplaced during sagduction (dome and basin structures). Their partial melting, with amphibole and garnet as residual phases, has been proposed for the genesis of the tonalites—diorites—granodiorites of the Miocene Cordillera Blanca batholith in Peru [24]. Such a process may have led to both the observed silica increase and REE crossover in the resulting lavas. Nevertheless, the necessary role of mantle material, as suggested by the presence of olivine with chromite inclusions in Licancabur lavas, and the high Mg, Ni, and Cr contents of the lavas (see below), would be more difficult to explain. Finally, if fractionation of garnet occurs in

mantle-derived primary magmas issued from partial melting of the mantle wedge, at the bottom of the continental crust where granulites are likely to be present, the fractionation of such granulite-type garnets ( $\approx \text{Prp}_{30}\text{Alm}_{60}\text{Sps}_{10}$ ) would affect the major element composition of these mantle-derived liquids usually of per- to meta-aluminous compositions [25]. Major element modelling indeed fails to give satisfactory results.

### 5.2. Mixing with partial melts derived from the overlying mantle wedge: the source of Mg-, Ni- and Cr-rich compositions

Since Gill [13], it is commonly admitted that overlying mantle wedge contributes predominantly (up to 90 wt %) to the calc-alkaline magmatism. Partial melting of the overlying mantle wedge is induced by the ascent of primary magmas and associated hydrous fluids, issued from the subducted plate. Whereas alumina basalts with olivine phenocrysts and their spinel inclusions predominate in northern, southern and austral Andes, they are quite absent in the CVZ, basaltic andesites ( $53 < \text{SiO}_2 \text{ wt } \% < 56$ ) being very scarce [9]. Nevertheless, these basaltic andesites contain olivine phenocrysts and xenocrysts ( $\text{Fo} > 80$  and  $\text{Fo} > 85$ , respectively) with Cr-spinel inclusions, a fact which corroborates their mantle origin. Furthermore, the high MgO, Ni and Cr contents of the andesites and dacites from the CVZ [8], when compared to those of lavas with equivalent  $\text{SiO}_2$  contents of the NVZ and SVZ, is another argument in favor of the implication of the mantle wedge during their genesis. Mixing of the slab-derived primary magmas with less than 10 wt % of mantle-derived liquids (melting rate  $\approx 1\%$ ) will give the observed MgO, Ni and Cr characteristics.

The REE crossover observed at Licancabur cannot be explained by a single and simple evolution through crystal fractionation of primary magmas issued from mantle partial melts. Normalized-REE diagrams are good indicators of amphibole and garnet fractionation which yields to middle- and heavy-REE depletions, respectively, in the evolved liquids. Amphibole and garnet fractionations must have played a role at Licancabur. Modelling of garnet fractionation gives satisfactory results ( $\sum r^2 < 0.1$ ) using a composition of typical garnet of eclogites ( $\text{Prp}_{55}\text{Alm}_{25}\text{Sps}_{20}$ ) as products of oceanic crust metamorphism. The composition of peridotite garnets ( $\text{Prp}_{70}\text{Alm}_{10}\text{Sps}_{20}$ ;  $\text{MgO} \approx 20 \text{ wt } \%$ ) is by far too different and does not lead to a convenient fractionation modelling.

### 5.3. Continental crust assimilation

The continental crust is 60–70 km thick in Licancabur area [29], but it is necessary to distinguish the possible role of the lower continental crust (deeper than 40 km) where magmas can be generated (as in the MASH model, [17]) from that of the upper continental crust (5–15 km depth) where magmas are stored and can evolve by crystal fractionation, mixing and assimilation.

#### 5.3.1. Lower crust assimilation: the clue to high Sr-isotope ratios

The role of the lower crust is still largely debated. The assimilation of lower crustal material will undoubtedly enhance incompatible element contents and Sr-isotope ratios in the contaminated magmas. It is likely that Archaean TTG of granodiorite composition [22] are present at the bottom of the Andean continental crust [5]. Low rate assimilation of these rocks will not significantly modify the trace and major element composition of Licancabur magmas. But these Archaean TTG do have very high present-day Sr-isotope ratios, probably as high as 0.820 [21], therefore, AFC modelling [7] indicates that the Sr-isotope composition of Licancabur magmas (estimated at  $\approx 0.704$ ) will increase up to 0.708 by assimilation of less than 1.0 wt % Archaean TTG. This value is lower than that (10 wt %) proposed by [4] for assimilation of Belen (North Chile) amphibolites and gneisses (0.5 to 1.0 Ga) by calc-alkaline Parinacota magmas.

#### 5.3.2. Upper crust assimilation?

The ignimbrite magmas, represented here by the Purico ignimbrite J32, are potential contaminants issued from the upper crust. Nevertheless this ignimbrite has numerous trace elements (Y, Ta, Ba, Sr, Th) that plot apart from the evolution trends for the Licancabur lava series (Fig. 3) and its HREE content is higher than those of all Licancabur lavas (but the basaltic andesite L31) which excludes a simple assimilation. Furthermore, the HREE content of the Purico ignimbrite (e.g. Yb: 1.91 ppm) is higher than those of all the Licancabur lavas (but the less differentiated) which excludes any possibility of crossing-over of the REE patterns. In a  $^{87}\text{Sr}/^{86}\text{Sr}$ - $\epsilon\text{Nd}$  diagram (not presented), the trend for Licancabur lavas present a concave pattern trending towards the Purico ignimbrite ( $^{87}\text{Sr}/^{86}\text{Sr}$ : 0.7087;  $\epsilon\text{Nd}$ : -7.5), this rock being isotopically close to lavas from the Licancabur upper unit. Surrounding gneisses and volcanic rocks of Devonian-Permian ages (unpublished data and [20]) are other potential candidates, but their

REE contents (La: 43 ppm, Yb: 4.8 ppm) are higher than those of all the Licancabur lavas, excluding any crossing over of the normalized patterns.

#### 5.4. Differentiation and evolution of magmas

The upper crust accommodates low pressure crystal fractionation and mixing between magmas of andesitic composition.

##### 5.4.1. Differentiation by crystal fractionation

The evolutions of both the composition and modal abundances of the phenocrysts are strong arguments in favor of crystal fractionation to explain the differentiation of the Licancabur lava series. Modelling for major elements gave results ( $\sum r^2 < 0.05$ ) in conformity with the observed mineralogy of the lavas (the calculations have been processed as in [10]). Evolution is thus fairly explained for andesites at Licancabur by fractionation of Ol + Pl + Cpx + Opx + Ti-Mag with  $\sum r^2 < 0.05$ . But for dacites, fractionation of the same phases + hornblende does not give satisfactory result ( $\sum r^2 < 0.45$ ). Furthermore, plagioclase phenocrysts are almost absent in dacites. For trace elements, measured/calculated ratios are between 0.8 and 1.1, the highest differences corresponding to Y and HREE [12]. Nevertheless this modelling alone does not explain the shape of the REE patterns and their crossover which should result from garnet  $\pm$  amphibole fractionation during the genesis of primary magmas.

##### 5.4.2. Evidence of mixing between magmas of andesitic composition

Numerous petrographical and mineralogical observations argue in favor of magma mixing during the differentiation of Licancabur magmas:

- occurrence in the same lava sample of limpid and sieve-textured plagioclase phenocrysts;
- alternatively normally and reversely zoned plagioclase and pyroxene phenocrysts;
- embayments of clinopyroxene phenocrysts;
- orthopyroxene corona around olivine phenocrysts;
- higher equilibrium temperatures for rims than for cores of pyroxene phenocrysts;
- occurrence of various phenocryst populations for both plagioclase and orthopyroxene in a given lava.

Although in Harker diagrams Licancabur lavas display rather linear evolution trends, incompatible—compatible element graphs do not allow one to confirm the role of mixing due to the lack of potential

contaminant end-members. More probably, mixing only concerns magmas with SiO<sub>2</sub> content in the 58–62 wt % range, and thus has a very limited role on the evolution of the series.

## 6. Conclusions

An appealing four step model is proposed for the genesis of the Licancabur adakite-like lavas (Fig. 6):

- partial melting (5 to 10 wt %) of an altered oceanic crust metamorphosed into garnet amphibolites and amphibole eclogites with a residual garnet  $\pm$  amphibole assemblage giving batches of primary magmas of andesitic and dacitic composition, respectively;
- the resulting primary magmas and their associated hydrous fluids induce partial melting (< 10 wt %) of the overlying lithospheric mantle wedge resulting in the genesis of hybrid magmas with high MgO, Cr and Ni contents;
- contamination ( $\approx$  1 wt %) of these hybrid magmas by TTG-type granodiorites of the Archean lower continental crust (with high present-day Sr isotopic ratio of 0.820). This process explains that Licancabur lavas have higher Sr-isotopic ratios than adakites but ratios similar to those of the Cenozoic CVZ calc-alkaline lavas ( $^{87}\text{Sr}/^{86}\text{Sr} \approx 0.707\text{--}0.708$ ) which were probably contaminated by the same process. The major and trace element compositions remain globally unaffected by this contamination process;
- evolution and differentiation of the derived individual magma batches by crystal fractionation (< 6 wt %) and late magma mixing (with compositions around 60 wt % SiO<sub>2</sub>) at upper crust levels.

## Acknowledgements

Financial support from ECOS (action C01U03 for travels and stays of B.D. and O.F.), from Lab. MAGIE (Dir. Prof. A. Jambon) UPMC Paris VI—UMR 7154, and from Dirección de Investigación de la Universidad de Concepción are greatly acknowledged. Isotopic measurements in ULB (Brussels) are partly funded by FNRS grants to D.D. Constructive reviews by J. Touret and an anonymous reviewer have been greatly appreciated. Contribution IPGP no. 2395.

## References

- [1] L.D. Ashwal, D. Demaiffe, T.H. Torsvik, Petrogenesis of Neoproterozoic granitoids and related rocks from the Seychel-

- les: the case for an Andean-type arc origin, *J. Petrol.* 43 (2002) 45–83.
- [2] E. Bourdon, J.-P. Eissen, M.-A. Gutscher, M. Monzier, P. Samaniego, C. Robin, C. Bollinger, J. Cotten, Slab melting and slab melt metasomatism in the northern Andean volcanic zone: adakite and high-Mg andesites at Pichincha volcano (Ecuador), *Bull. Soc. Geol. France* 173 (2002) 195–206.
- [3] E. Bourdon, J.-P. Eissen, M. Monzier, C. Robin, H. Martin, J. Cotten, M.L. Hall, Adakite-like lavas from Antisana volcano (Ecuador): evidence for slab melt metasomatism beneath the Andean Northern Volcanic Zone, *J. Petrol.* 43 (2002) 199–217.
- [4] E. Bourdon, G. Wörner, A. Zindler, U-series evidence for crustal involvement and magma residence times in the petrogenesis of Parínacota volcano, Chile, *Contrib. Mineral. Petrol.* 139 (2000) 458–469.
- [5] B. Dalmeyrac, J.R. Lancelot, A. Leyreloup, Two-billion-year granulites in the Late Precambrian metamorphic basement along the southern Peruvian coast, *Science* 198 (1977) 49–51.
- [6] J. Defant, M.S. Drummond, Derivation of some modern arc magmas by melting of subducted lithosphere, *Nature* 347 (1990) 662–665.
- [7] D.J. DePaolo, Trace element and isotopic effects of combined wallrock assimilation and fractional crystallization, *Earth Planet. Sci. Lett.* 53 (1981) 189–202.
- [8] B. Déruelle, Petrology of the Plio-Quaternary volcanism of the South-Central and Meridional Andes, *J. Volcanol. Geothermal Res.* 14 (1982) 77–124.
- [9] B. Déruelle, O. Figueroa, Insights into the upper mantle from basalts from the Chilean Altiplano, South-Central Andes, 8° Congr., Geol. Chileno, Antofagasta, Chile, *Actas* 2 (1997) 317–321.
- [10] B. Déruelle, L.E. López, Basaltes, andésites, dacites et rhyolites des strato-volcans des Nevados de Chillán et de l'Antuco (Andes méridionales): la remarquable illustration d'une différenciation par cristallisation fractionnée, *C.R. Acad. Sci. Paris Ser. IIA* 329 (1999) 337–344.
- [11] S.L. De Silva, Geochronology and stratigraphy of the ignimbrites from the 21°30' S to 23°30' S portion of the central Andes of northern Chile, *J. Volcanol. Geothermal Res.* 37 (1989) 93–131.
- [12] O. Figueroa, *Pétrologie du volcan Licancabur (zone volcanique des Andes centrales)*. Thèse, université Pierre-et-Marie-Curie, Paris, 2001, 209 p.
- [13] J. Gill, *Orogenic andesites and plate tectonics*, Springer-Verlag, Berlin, 1981.
- [14] T.H. Green, Experimental studies of trace-element partitioning applicable to igneous petrogenesis—Sedona 16 years later, *Chem. Geol.* 117 (1994) 1–36.
- [15] T.H. Green, A.E. Ringwood, Genesis of calc-alkaline igneous rock suite, *Contrib. Mineral. Petrol.* 18 (1968) 105–162.
- [16] R.S. Harmon, B. Barreiro, S. Moorbath, J. Hoefs, P.W. Francis, R.S. Thorpe, B. Déruelle, J. Mc Hugh, J.A. Vigliano, Regional O-, Sr-, and Pb-isotope relationships in Late Cenozoic calc-alkaline lavas in the Andean Cordillera, *J. Geol. Soc.* 141 (1984) 803–822.
- [17] W. Hildreth, S. Moorbath, Crustal contributions to arc magmatism in the Andes of Central Chile, *Contrib. Mineral. Petrol.* 98 (1988) 455–489.
- [18] C. Kull, F. Hänni, M. Grosjean, H. Veit, Evidence of an LGM cooling in NW-Argentina (22°S) derived from a glacier climate model, *Quaternary Int.* 108 (2003) 3–11.
- [19] B.E. Leake (chairman) and 20 co-authors, Nomenclature of amphiboles: report of the Subcommittee on amphiboles of the International Mineralogical Association Commission on new minerals and mineral names, *Mineral. Mag.* 61 (1997) 295–321.
- [20] F. Lucassen, G. Franz, A. Laber, Permian high pressure rocks—the basement of the Sierra de Limón Verde in northern Chile, *J. South Am. Earth Sci.* 12 (1999) 183–199.
- [21] F. Lucassen, R. Becchio, R. Harmon, S. Kasemann, G. Franz, R. Trumbull, H.-G. Wilke, R.L. Romer, P. Dulski, Composition and density model of the continental crust at an active continental margin—the central Andes between 21° and 27°S, *Tectonophysics* 341 (2001) 195–223.
- [22] H. Martin, Petrogenesis of Archaean trondhjemites, tonalites and granodiorites from eastern Finland: major and trace element geochemistry, *J. Petrol.* 28 (1987) 921–953.
- [23] W.F. McDonough, S. Sun, The composition of the Earth, *Chem. Geol.* 120 (1995) 223–253.
- [24] N. Petford, M. Atherton, Na-rich partial melts from newly underplated basaltic crust: the Cordillera Blanca batholith, Peru, *J. Petrol.* 37 (1996) 1491–1521.
- [25] O. Müntener, R. Perez-Alonso, P. Ulmer, Phase relations of garnet, amphibole and plagioclase in H<sub>2</sub>O undersaturated andesite liquids at high pressure and implications for the genesis of lower arc crust, *Geophys. Res. Abstr.* 6 (2004) 05183.
- [26] R.P. Rapp, N. Shimizu, M.D. Norman, G.S. Applegate, Reaction between slab-derived melts and peridotite in the mantle wedge: experimental constraints at 3.8 GPa, *Chem. Geol.* 160 (1999) 335–356.
- [27] C.R. Stern, R. Kilian, Role of subducted slab, mantle wedge and continental crust in the generation of adakites from the Andean Austral Volcanic Zone, *Contrib. Mineral. Petrol.* 123 (1996) 263–281.
- [28] The ANCORP Working Group, Seismic reflection image revealing offset of Andean subduction-zone earthquake locations into oceanic mantle, *Nature* 397 (1999) 341–344.
- [29] P.J. Wigger, M. Schmitz, M. Aráneda, G. Asch, S. Baldzuhn, P. Giese, W.-D. Heinsohn, E. Martínez, E. Ricaldi, P. Röwer, J. Viramonte, Variation in the crustal structure of the southern central Andes deduced from seismic refraction investigations, in: K.-J. Reutter, E. Scheuber, P.J. Wigger (Eds.), *Tectonics of the southern central Andes*, Springer-Verlag, Berlin, 1994, pp. 23–48.